MIT Libraries | DSpace@MIT

MIT Open Access Articles

Photoelectrochemical synthesis of DNA microarrays

The MIT Faculty has made this article openly available. ***Please share*** how this access benefits you. Your story matters.

Citation: Chow, Brian Y, Christopher J Emig, and Joseph M Jacobson. "Photoelectrochemical synthesis of DNA microarrays." Proceedings of the National Academy of Sciences 106.36 (2009): 15219-15224. © 2009 National Academy of Sciences

As Published: http://dx.doi.org/10.1073/pnas.0813011106

Publisher: United States National Academy of Sciences

Persistent URL: http://hdl.handle.net/1721.1/55288

Version: Final published version: final published article, as it appeared in a journal, conference proceedings, or other formally published context

Terms of Use: Article is made available in accordance with the publisher's policy and may be subject to US copyright law. Please refer to the publisher's site for terms of use.

Massachusetts Institute of Technology

Photoelectrochemical synthesis of DNA microarrays

Brian Y. Chow[1], Christopher J. Emig[2], and Joseph M. Jacobson[3]

The Center for Bits and Atoms, The Media Laboratory, Massachusetts Institute of Technology, 20 Ames Street, Cambridge, MA 02139

Edited by Alexander Rich, Massachusetts Institute of Technology, Cambridge, MA, and approved June 11, 2009 (received for review December 19, 2008)

Optical addressing of semiconductor electrodes represents a powerful technology that enables the independent and parallel control of a very large number of electrical phenomena at the solid-electrolyte interface. To date, it has been used in a wide range of applications including electrophoretic manipulation, biomolecule sensing, and stimulating networks of neurons. Here, we have adapted this approach for the parallel addressing of redox reactions, and report the construction of a DNA microarray synthesis platform based on semiconductor photoelectrochemistry (PEC). An amorphous silicon photoconductor is activated by an optical projection system to create virtual electrodes capable of electrochemically generating protons; these PEC-generated protons then cleave the acid-labile dimethoxytrityl protecting groups of DNA phosphoramidite synthesis reagents with the requisite spatial selectivity to generate DNA microarrays. Furthermore, a thin-film porous glass dramatically increases the amount of DNA synthesized per chip by over an order of magnitude versus uncoated glass. This platform demonstrates that PEC can be used toward combinatorial bio-polymer and small molecule synthesis.

combinatorial chemistry | genomics | opto-electronics | phosphoramidite | solid-phase synthesis

The opto-electronic properties of semiconductor electrodes (1, 2) make them powerful and versatile tools for light-driven biological applications. By irradiating the surface with a spatially modulated light source to lower the impedance at the illuminated areas, virtually-addressable electrodes can be created that greatly limit the amount of device fabrication required for complex and addressable electrode architectures. Furthermore, the photocurrent that passes through the electrode can be heavily influenced by the local chemical environment. These properties have been leveraged in the photoelectrochemical sensing of biomolecules and enzymatic activity (3, 4), photoelectrophoretic transport to physically manipulate biomolecules and cells (5–7), and photoelectrical stimulation of electrophysiological activity (8, 9). Here, we report a DNA microarray synthesis platform based on the principles of semiconductor photoelectrochemistry (PEC), demonstrating that semiconductor electrodes and PEC can be used toward in situ combinatorial chemistry and biopolymer synthesis.

The crux of any in situ microarray fabrication technology is the ability to perform a chemical addition or protecting group removal step with spatial selectivity. This selectivity has previously been achieved by a variety of methods, such as ink-jet printing (10, 11), UV photocleavage (12–14), photo-generating acids (15, 16), electrochemically generating acids (17, 18), and electrophoretic delivery of reagent-embedded dielectric particles (19). The PEC platform reported here (Fig. 1) uses light to gate the electrochemical generation of protons at a semiconductor anode that is addressed by a digital micromirror device (DMD). These protons then cleave the acid-labile dimethoxytrityl (DMT) protecting groups of standard phosphoramidite reagents at the virtual electrode.

The principles behind the ability to selectively generate protons upon illumination are also shown in Fig. 1. When an n-type semiconductor anode is illuminated with light above its bandgap energy (E_g), valence band electrons are photo-excited into the conduction band, which creates valence band holes that can participate in an oxidation reaction (Fig. 1*A*). The holes are driven toward the surface by the applied electrical bias, where they recombine with electrons generated in solution by the reaction and transferred via the metal layer. The anodic reaction of interest liberates protons by the oxidation of hydroquinone to benzoquinone. Strong illumination can also increase the reaction efficiency at the illuminated surface, by raising the surface potential at the solid electrolyte interface (SEI), or in other words, by lowering the applied bias potential drop across the semiconductor (Fig. 1*B*) (1, 2).

We discuss the design and fabrication of an amorphous silicon-based photoconductive anode, that was characterized by both solid-state and photoelectrochemical methods, and whose properties were critical to the success of the microarray synthesis platform. Successful microarray synthesis was demonstrated by hybridization of fluorescently-labeled oligonucleotides. Also developed was an optically transparent thin-film porous glass coating that dramatically increases the amount of DNA produced per chip by over an order of magnitude. This work could lead to the creation of a flexible and integrated platform in which biological molecules are synthesized, manipulated, and sensed using the same virtually addressed, light-activated semiconductor electrode.

Results

Photoconductor Fabrication and Characterization. From bottom to top, the photoconductive anode (Fig. 1*C*) is composed of indium tin oxide-coated glass (ITO-glass) as the rear electrical contact, 1 μm-thick undoped amorphous silicon (a-Si), and 100 nm-thick platinum pads (with 15 nm-thick titanium adhesion layers). Amorphous silicon was chosen as the photoconductive material because given its narrow bandgap (E_g = 1.7 eV), mobile charge carriers can be generated with visible light instead of UV light, the latter of which requires more expensive optics. The inert platinum layer improves electrical stability by preventing the thermal and chemical oxidation of a-Si into an insulating oxide. A thin-film porous glass made from colloidal silica coats the entire substrate and increases the loading capacity of the chip with its large internal surface area. In contrast to addressable complementary metal oxide semiconductor (CMOS) electrodes that often require over 30 mask steps to fabricate, the entire device here can be cheaply fabricated with a single, unaligned mask step. It should be noted that not all photoconductors are suitable for PEC synthesis, and that the nature of the substrate fabricated here was critical to the success of the system, as will later be discussed.

To understand the nature of the photoconductor, extensive solid-state and PEC analyses were performed. Diode measure-

Author contributions: B.Y.C., C.J.E., and J.M.J. designed research; B.Y.C. and C.J.E. performed research; and B.Y.C., C.J.E., and J.M.J. wrote the paper.

The authors declare no conflict of interest.

This article is a PNAS Direct Submission.

[1]Present address: The Media Laboratory and Department of Biological Engineering, Massachusetts Institute of Technology, Cambridge, MA 02139.

[2]Future address: Department of Bioengineering, Stanford University, Stanford, CA 94305.

[3]To whom correspondence should be addressed. Email: jacobson@media.mit.edu.

This article contains supporting information online at www.pnas.org/cgi/content/full/0813011106/DCSupplemental.

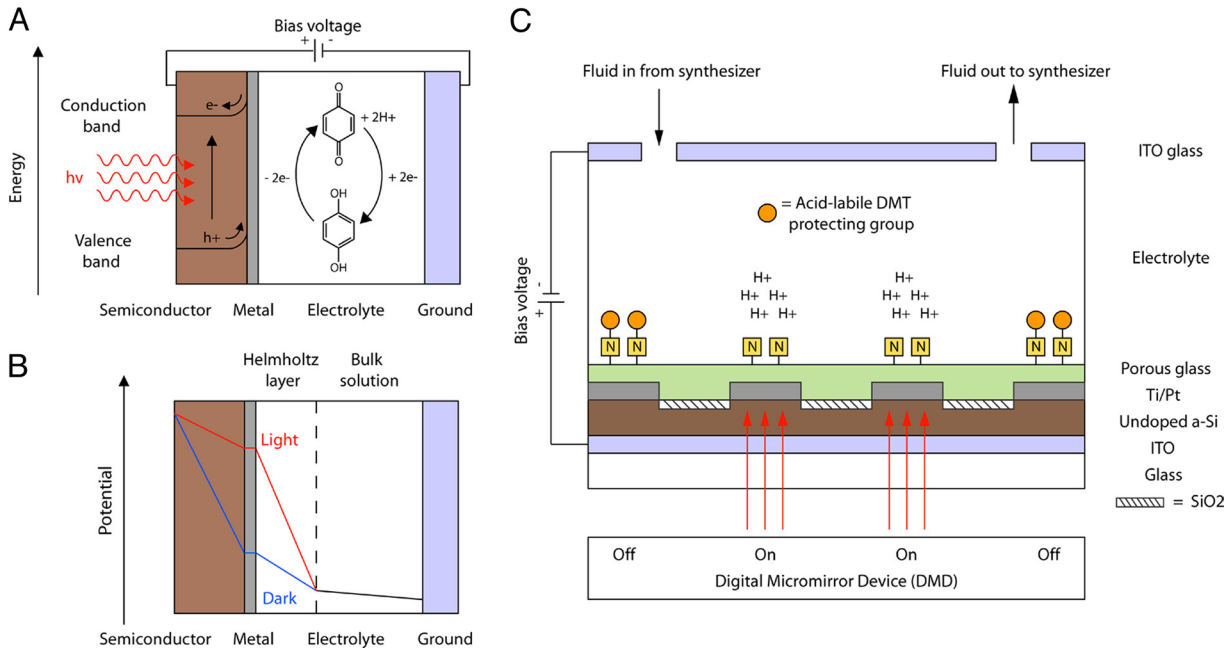

Fig. 1. Principles of PEC microarray synthesis. (*A*) Band diagram of the PEC cell. Illuminating the semiconductor electrode photogenerates charge carriers that can participate in the oxidation of hydroquinone to liberate protons. (*B*) Potential profile of illuminated (''light'') and nonilluminated (''dark'') PEC cells. The light electrode has a much higher surface potential at the SEI, making it a more efficient electrochemical anode. (*C*) Schematic of the proposed PEC synthesis platform, showing site-selective cleavage of acid-labile protecting groups by PEC-generated protons. For simplicity, the growing strand is only drawn on top of the thin-film porous glass, but the synthesis occurs throughout the film.

ments showed that the substrate behaves like a very lightly doped n-type Schottky diode that generates photopotentials as large as +205 mV above 500 mW/cm^2 illumination power [*SI Text* (Supporting Note 1) and Fig. S1]. Fig. 2*A* shows a cyclic voltammogram (C-V) of 2.5 mM hydroquinone with 100 mM tetrabutylammonium hexafluorophosphate salt in acetonitrile, taken using the a-Si photoconductor as a light-activated working electrode versus a platinum quasi-reference electrode (QRE) (see ref. 20 for an explanation of voltammetric methods). The "light" and "dark" substrates were irradiated with 1 W/cm^2 and 1 mW/cm^2 white light, respectively. The PEC oxidation rates increase upon illumination, as proposed in Fig. 1*A*. Notice that a characteristic mass transport-limited peak is observable in the light C-V (asterisk in Fig. 2*A*), but no such peak is observable in the dark C-V (*Inset*). Fig. 2*B*, which plots the relative potential drop across the semiconductor and electrolyte of the SEI ($\Delta\Phi/\Phi_{bias}$) versus illumination intensity, shows that the surface potential at the SEI is larger in the light state, as proposed in Fig. 1*B*.

Microarray Synthesis. "Dose tests" measuring deprotection efficiency of the acid-labile DMT group vs. illumination time were assayed by coupling Cy3-phosphoramidite and fluorescence quantification by confocal fluorescence microscopy (Fig. 3*A*). Electrochemical solutions were composed of 100 mM hydroquinone with 100 mM tetrabutylammonium hexafluorophosphate in acetonitrile. The substrates were biased at + 1.7 V with respect to ground and illuminated at 1 W/cm^2 white light. Complete deprotection or detritylation was achieved without noticeable acid diffusion halos typically between 20–28 s. Variations exist between pads due to nonuniformities in the optical field and the porous glass (e.g., pinholes, film thickness).

Such a time window during which the protons are spatially confined to the electrode presumably exists because the proton diffusion profile is anisotropic, with the preferred direction away from the surface rather than laterally along it (20). Although our data confirms that the initial profile is indeed highly anisotropic [*SI Text* (Supporting Note 2) and Fig. S2], it is unclear whether the spatial confinement is lost because an accumulation layer grows thick enough for the diffusion profile to become isotropic, or merely broadens (i.e., still anisotropic). As will be shown, the anisotropy provides sufficient proton containment to successfully synthesize a DNA microarray, but future versions will likely require increased control over the diffusion of reactive species, some options for which are discussed later.

Fig. 3*B* shows a fluorescence intensity map of Cy3-phosphoramidite coupled to the surface after one 22-s detritylation step, spelling "MIT." Control experiments were performed to verify that this selective coupling indeed resulted from selective detritylation by PEC-generated acids, as opposed to direct electrochemical protecting group removal or damage to the growing strand [*SI Text* (Supporting Note 3) and Fig. S3]. Once suitable detritylation conditions were determined, microarrays were synthesized and assayed by the hybridization of fluorescently labeled oligonucleotides. Two different 12-mers were synthesized in a checkerboard pattern, where the middle 2 base positions contain the exact same match/mismatch combination to the complementary pair of targets (AT or TA). Each spot is perfectly complementary to 1 target strand in solution, and contains both A-A and T-T mismatches to the other. Fig. 4*A* shows the fluorescence image of the substrate after simultaneous hybridization of both target molecules labeled at the 3′-end with Cy3 or fluorescein dyes, demonstrating successful microarray synthesis.

The average stepwise yield was determined by methods similar to those previously described to measure the stepwise yield using photocleavable reagents (21, 22). Briefly, oligonucleotides of varying lengths, from 1 to 10 bases, were first randomly PEC synthesized (mixture of equal parts dA, dG, dC, and dT phosphoramidites). Next, Cy3-phosphoramidite was coupled to the entire chip after treatment with commercial halo-acid deblocking solution, and finally, the average stepwise yield was calculated based on the fluorescence signal intensity of each N-mer,

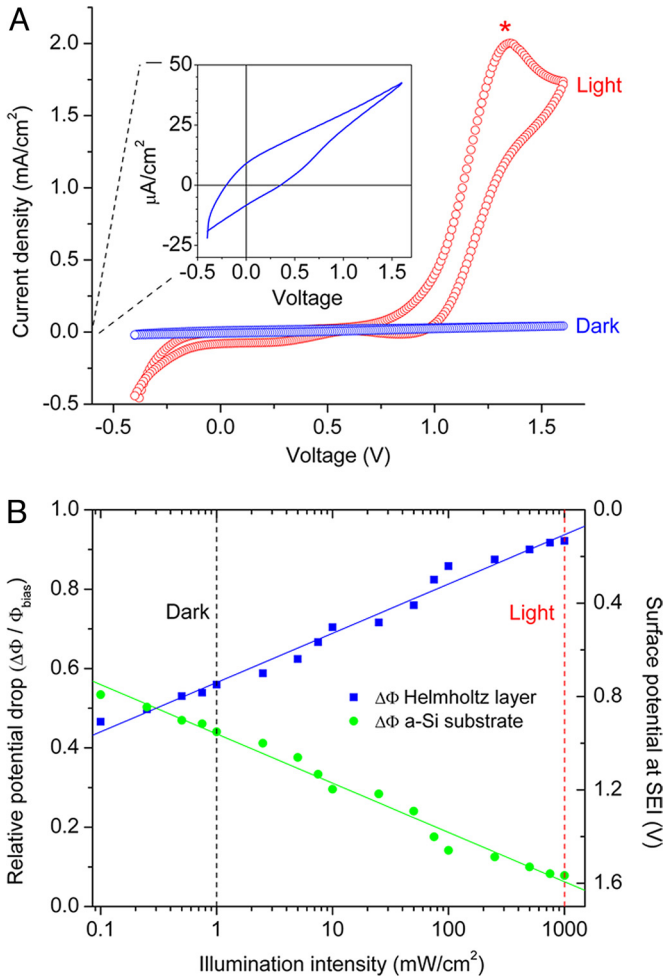

Fig. 2. PEC characterization of the substrate. The ''light'' and ''dark'' states have been illuminated with 1 W/cm2 and 1 mW/cm2 white light, respectively. (*A*) Cyclic voltammogram (C-V) of 2.5 mM hydroquinone with 100 mM salt in acetonitrile. A diffusion- or mass transport-limited peak is observable (red asterisk) in the light state, whereas no such peak can be seen in the dark state (*Inset*). (*B*) Relative potential drops across the SEI (left ordinate) and measured electrode surface potential (right ordinate) as a function of illumination intensity. A 1.7-V bias was applied across the PEC cell. *A* and *B* verify the mechanisms proposed in Fig. 1 *B* and *C*, respectively.

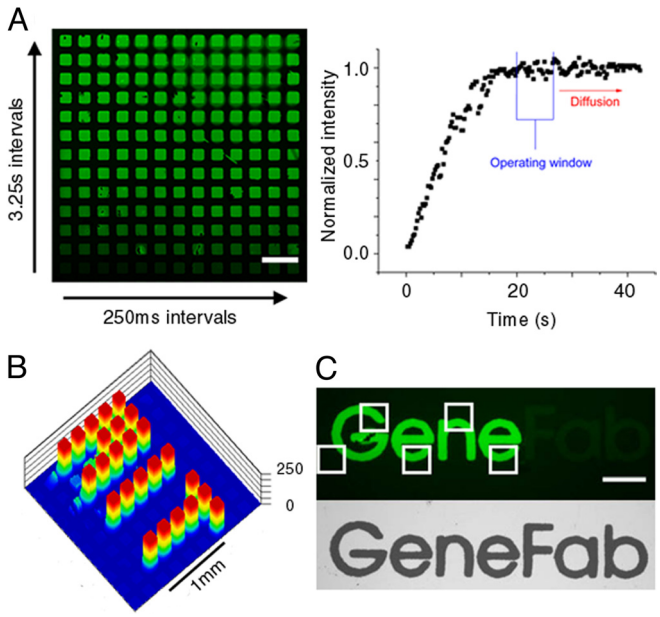

Fig. 3. Fluorescence analysis of selective PEC detritylation. All substrates were biased at +1.7 V, using a deprotection solution of 100 mM hydroquinone and 100 mM salt in acetonitrile. The fluorescence in all images originates from direct Cy3-phosphoramidite coupling to surface-bound DMT-dT molecules after PEC detritylation. (*A*) ''Dose tests'' to determine the optimal detritylation times (*Left*). Complete deprotection is achieved without loss of spatial confinement of protons in an operating window between 20–28 s, after which noticeable diffusion occurs. Normalized deprotection efficiency vs. time was determined from emission readings (*Right*). (*B*) Fluorescence intensity display after one 22-s detritylation step spelling ''MIT.'' (*C Upper*) The sharpness is largely defined by the metal patterning. Even though the electrode spelling was only partially illuminated (boxes), the detritylation was still spatially uniform because the metal spreads the charge. (*Lower*) An optical image of the mask is provided to aid the eye. (Scale bars: *A*, 400 μm; *C*, 200 μm.)

normalized against adjacent spots that were never illuminated. The stepwise yield (Fig. 4*B*) rose from 90% for strand length n = 1 to ≈93% after n = 5. This trend, in which the stepwise yield is particularly poor at first and then stabilizes after several base additions, has also been reported (21) or can be inferred from the data of others (22). The 93% stepwise yield is in line with previous first reports, which have ranged from 91–98% (21–25). Future studies will aim to optimize system parameters by constructing an improved optical projection system, examining other suitable semiconductors and device architectures (e.g., nanoparticle-based films, *n-i-p* diodes, microfabricated fluidic channels), and altering the coupling cycles (16, 26).

A notable aspect of the synthesis platform is that the sharpness of the synthesis area is largely defined by the metal pad itself. In UV-photocleavage platforms, the spatial uniformity of protecting group removal corresponds to the uniformity of the optical field (27). Thus, optical misalignment and drift directly result in synthesis errors in such a system. However, if only part of the metal pad is illuminated in the PEC system, the deprotection is still spatially uniform (so long as the porous glass is uniform) because the metal pads spread the charge carriers. Fig. 3*D* shows Cy3-phosphoramidite coupled to prepatterned electrodes that spell ''GeneFab.'' Even though the letters in ''Gene'' were only partially illuminated at the locations indicated by the boxes, the fluorescence is homogenous across the pad. The lateral electron spreading relaxes the image locking requirements (27) to maintain spatial homogeneity of the acid PEC-generation, although it is important to note that image locking is still extremely important for the beam to maintain registration with the metal pads, particularly at high spot densities.

Porous Glass Characterization. The porous glass film that coats the surface could benefit other microarray technologies, as well as chemical sensing applications that require a large-pore immobilization matrix (28). It can easily be formed on virtually any substrate with tunable thicknesses (75 nm–1.4 μm) in a 1-step spin-coating process (Fig. S4). It is optically transparent with >98% transmission from 350–700 nm (Fig. S4). The pores were typically 15–85 nm in diameter, as determined by low-voltage scanning electron microscopy and atomic force microscopy (Fig. S4). The current density during cyclic voltammetry using a coated electrode was ≈60% of the value from an uncoated one (Fig. S4).

The film is necessary to physically space the DNA from the electrode surface to limit direct electrochemical damage to the growing DNA strands and surface linker molecules. However, perhaps the most interesting property of the film is its large surface area that increases the oligonucleotide concentration per spot (i.e., amount of DNA synthesized per chip) by emulating

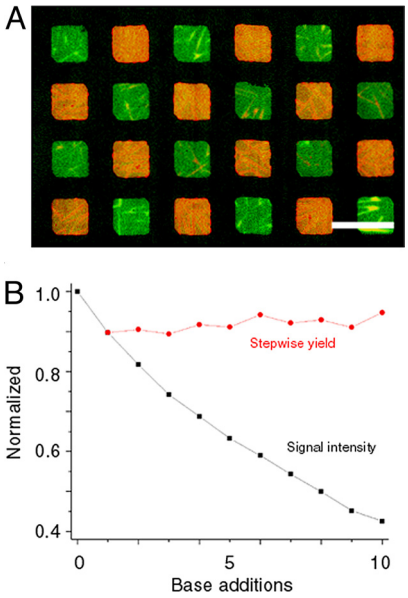

Fig. 4. Fluorescence analysis of PEC microarray synthesis. (*A*) Checkerboard pattern of 2 12-mer probes with identical mutations at the middle 2 positions. The substrate was simultaneously hybridized to Cy3- and fluorescein-labeled targets (fluorescein in green), each having 1 match and 1 mismatch probe on the surface. (*B*) Stepwise synthesis yield determined from the fluorescence signal emanating from direct Cy3-phosphoramidite coupling after n = 1–10 nonfluorescent base additions. The stepwise yield reaches a steady-state ≈93% after a few base additions.

A

Substrate	Dimethoxytrityl cation		40-mer (0.2umol cycle)	
	Area density (molecule/cm2)	Conc (mM)	Area density (molecule/cm2)	Conc. (mM)
Flat glass (unpolished)	$1.8 \pm 0.1 \times 10^{14}$	N/A	$1.9 \pm 0.3 \times 10^{13}$	N/A
Porous oxide (~840nm)	$1.3 \pm 0.2 \times 10^{16}$	25.0 ± 2.8	$2.5 \pm 0.2 \times 10^{14}$	4.7 ± 0.4
Controlled pore glass (0.2umol)	$1.8 \pm 0.1 \times 10^{14}$	13.2 ± 0.3	N/A	5.9 ± 0.2

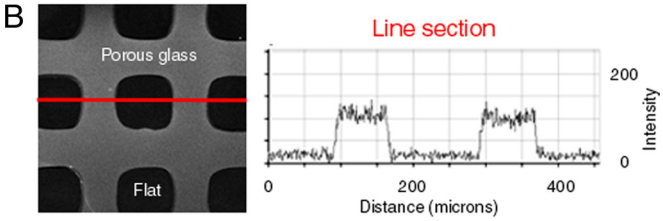

Fig. 5. DNA synthesis capacity enhancement using a porous glass film (840 nm thick) with large internal surface area. (*A*) UV-vis spectroscopic quantification of molecules cleaved from the film to determine surface loading within the film. All DNA was synthesized with a standard 0.2-μmol phosphoramidite cycle. (*B*) Posthybridization fluorescence image demonstrating the signal enhancement from the film. Wells were etched to expose the bare glass under the film, and then a 30-mer was synthesized simultaneously on the exposed flat glass and porous film. After the Cy3-labeled complementary strand was hybridized to the substrate, the fluorescence from the grid represents the relative increase in signal intensity over a typical microarray. The relative increases are consistent between *A* and *B*.

controlled-pore glass. Although porous films have previously been used with microarrays to enhance fluorescence hybridization signal and sensitivity (29, 30), the film reported here was more robust and permitted larger electrochemical current densities. UV-Vis absorbance analysis of cleaved molecules showed an 87-fold increase per μm film thickness in the initial loading density of 5′-O-DMT-2′-dT-3′-O-succinate (DMT-dT-succinate), as well as a 16-fold (also per μm thickness) increase in 40-mers synthesized with a standard synthesis cycle after desalting (Fig. 5*A*). Note that the area density was defined with respect to 2-dimensional chip area (not available surface area), and that the concentration was defined with respect to the geometric volume of the film. It should be noted that the measured value of 1.9×10^{13} molecules/cm^2 on flat glass is quite high compared with typically reported values of approximately 2×10^{12} molecules/cm^2, although several others have reported similar or even higher values (see ref. 23 for a list of reported densities). The measured density is most likely large because the unpolished glass used in this work has more microscopic surface area than typical microarray glass that is polished to near-atomic flatness.

The synthesis yield of 2.5×10^{14} molecules/cm^2 (or 415 pmol/cm^2) using the porous glass film means that a microarray (equal size spots and spacing) on a 1 inch × 3 inch coated microscope slide would produce over 2 nmol DNA (the unpatterned synthesis area reported here produced 325 pmol). To put this yield increase into perspective, Fig. 5*B* shows the difference in fluorescence intensity one would see between hybridization assays on coated and uncoated glass. Wells were buffered-oxide etched to expose the bare glass of a coated slide, and then a 30-mer was synthesized on the patterned substrate using standard synthesis procedures. Therefore, after hybridizing the complementary Cy-3 labeled oligonucleotide, the relative ratio of fluorescence intensity between the wells and the crossroads of the grid represents the signal difference between uncoated and coated glass, respectively.

Discussion

Although several light-addressable electrodes have been demonstrated for biomolecule sensing and manipulation (3, 5–7), the properties of the one reported here were critical to the success of the system. Very few semiconductor films that were tested actually succeeded for PEC synthesis. Testing of various a-Si deposition conditions, pad compositions (TiO_2, Pd, and Pt without an adhesion layer), and other semiconductor films (including silicon wafers of various doping, thin-film sputtered TiO_2, and spun-coat CdSe quantum dots) led to 2 empirical requirements for success. First, the film resistivity when illuminated must be relatively low ($R < \approx 10^5$ Ω·cm) at the applied bias to ensure reasonably short deprotection times. Likewise, the thickness of silicon wafers precluded their use due to the resultant high impedance and shallow penetration of light. Second, the surface defect density must not be large enough to impede the PEC reaction by creating barriers to hole-injection into solution (1, 2).

As previously mentioned, the chemical gradient and applied electric field create an anisotropic diffusion profile that kept PEC-generated protons sufficiently localized to the electrode of interest. However, future research will need to further address the control of proton diffusion, especially as the electrode size approaches "ultra-microelectrode" regime (typically <10 μm) (20), in which the diffusion is always isotropic. Several strategies could be beneficial to implement. Pulsed illumination could limit the accumulation layer by allowing protons to move away from the surface during a brief dark period when none are PEC-generated. This reduced accumulation would then limit the driving force for lateral diffusion between spots. Another useful strategy would be "inverse capping" (27), in which the areas between the spots are selectively deprotected and chemically capped before microarray synthesis, effectively setting a boundary beyond which there are no reactive groups. Inverse capping would reduce errors or halos by significantly increasing the distance the proton would have to diffuse before an unwanted detritylation.

Among the electrochemical DNA microarray synthesis platforms (17, 31), the use of proton scavengers is popular. Scavengers can be electrochemically generated by placing the ground electrode in between the pads (i.e., crossroads to a grid) to create a chemical wall that contains the protons. This strategy was initially attempted in this work using benzoquinone, which can be reduced to a proton-consuming radical at the ground/counter electrode. However, it was not pursued because of the extra microfabrication steps required. Weakly basic scavengers can also be placed in solution to slow down proton diffusion (31). This strategy was also initially attempted in this work (Fig. S3), but inclusion of the weak base in the deprotection solution quickly degraded the hydroquinone.

An interesting feature of a microarray platform based on PEC is increased generality versus other light-driven DNA microarray platforms, which in practice provide the highest spot densities. In context of more general combinatorial chemistry, chemically labile protecting groups are by far more varied and widely used than photolabile groups, as well as significantly cheaper in biopolymer synthesis. Considering that electrochemical protecting group removal has been demonstrated in biomolecule synthesis and surface-immobilization by electro-reduction (32), -oxidation (33), -catalysis (34, 35), and -generation of acids and bases (17, 18), PEC-gated reactions should be applicable to the in situ combinatorial synthesis of other biopolymers and small molecules.

The flexibility of semiconductor PEC also makes it attractive as a basis for a solid-phase combinatorial synthesis platform. A compelling future application would be the construction of a highly versatile, integrated biomolecule synthesis, manipulation, and biosensing platform. Photoelectrophoretic transport (5–7) has already been demonstrated to influence DNA hybridization rates and stringency (6). PEC is also a powerful tool in chemical sensing. Both label-free (3) and dye-sensitized (4) PEC biomolecule detection schemes have been reported, in which surface bound biomolecules alter the photocurrent through the irradiated semiconductor electrode. Thus, one could imagine that a properly designed PEC platform could be used to first synthesize the microarray, then improve the rate and stringency of target strand hybridization at illuminated areas (6), and finally to detect the hybridization event as a light-addressable electrochemical sensor. For example, Fig. 2 demonstrates the capability for the chip to serve as a virtually addressed electrochemical sensor; C-V's with single virtual-electrode resolution have also been recorded, but with currently insufficient signal-to-noise ratio to report here.

The large synthesis capacity of the porous glass film may greatly benefit applications that use custom microarrays to drive down the cost per base for genomic research, such as multiplexed gene synthesis (16, 26, 36), library construction (37, 38), and genomic selection for targeted sequencing (39–41). It effectively further lowers the cost per base by reducing the spot redundancy required to obtain biologically relevant quantities of each sequence, and also limits the need for amplification protocols. The use of a high-loading support may become increasingly important as the complexity of the DNA pool increases, because the quantity of each sequence decreases with the spot area. It should be noted that parallel gene synthesis in microfluidic devices may also address issues associated with the minute quantities of DNA obtained from cleaved microarrays (42).

In conclusion, we have successfully created a DNA microarray synthesis platform, demonstrating that photoelectrochemistry can be used toward combinatorial solid-phase chemical synthesis. In addition to optimizing the synthesis platform, future work may include the synthesis of other bio-polymers and small molecules, as well as the construction of an integrated platform that uses photoelectrochemistry to not only synthesize microarrays, but also to manipulate and detect target molecules in a massively parallel fashion.

Materials and Methods

All DNA synthesizer reagents were used as received from Glen Research (''Ultramild'' phosphoramidites), and all other reagents were from Aldrich, unless specified otherwise. Millipore-purified water (18.5 MΩ·cm) is denoted as dH_2O.

Substrate Fabrication. 1 μm thick undoped amorphous silicon films were deposited by plasma enhanced chemical vapor deposition (PECVD) at 250 °C with a PlasmaTherm 700 Series PECVD on top of ITO-glass (Delta Technologies, 0.7 mm thick, 15 Ω·sq). The electrodes were lithographically defined using AZ4620 photoresist (AZ Electronic Materials) exposed through transparency masks (Pageworks) on a Karl Suss MJB3 system. One hundred nanometer-thick platinum electrodes with 15 nm-thick titanium adhesion layers were deposited with a Sloan PAK-8 electron beam evaporator. After the photoresist was lifted-off in acetone and 1-methyl-pyrolidone, the substrate was oxygen plasma cleaned (Anatech, 100 mTorr, 50 sccm, 50 W) for 10 min to remove any residual photoresist and oxidize the exposed amorphous silicon.

Porous glass films (840 nm-thick) were deposited by spin-coating (2,500 rpm, 40 s). commercially available colloidal silica solutions (Snowtex UP or OUP). Films were then annealed on a hotplate at 400–420 °C for 1 h to improve film stability, and then slowly cooled to room temperature. Substrates were recovered by stripping the surface-immobilized molecules with freshly prepared 1× Nochromix (Godax Laboratories) in concentrated sulfuric acid for 1 h, or by stripping the entire porous glass by buffered oxide etching (BOE) and subsequently redepositing the film.

Reaction Apparatus. A flow-through cell was used to adapt an ABI 394 DNA synthesizer for the microarray platform (Fig. S5). ITO-glass was used as both the counter electrode and top portion of the cell. The optical projection system was constructed by modifying a digital light projector (DLP, Optoma EP719), by using a telescoping lens train (Fig. S6) to focus the output, down to 5-μm individual pixel sizes. The output power was ≈1 W/cm^2 white light in the ''on'' state, with a 950:1 contrast ratio. All components were from Thor Labs, except for the optical shutter (Uniblitz). Custom control and automation software was written in Python.

Oligonucleotide Microarray Synthesis. Before synthesis, substrates were silanized with 0.5% N-(3-triethoxysilylpropyl)-4-hyrdoxybutyramide (Gelest) in ethanol for 2 h. The free hydroxyl groups were protected by soaking the substrates in 50 mM 4,4′-dimethoxytrityl chloride and 50 mM triethylamine in toluene for 4 h under nitrogen. An ABI 394 synthesizer was used as the reagent manifold for DNA synthesis. The PEC detritylation mixture was composed of 100 mM hydroquinone and 100 mM tetrabutylammonium hexafluorophosphate salt in anhydrous acetonitrile. During the PEC detritylation step, the amorphous silicon substrate was biased at +1.7 V and irradiated for 22 s at 1 W/cm^2 white light. Following synthesis, the substrates were deblocked by soaking in 50 mM potassium carbonate in methanol for 6 h.

Hybridization Assays and Fluorescence Analyses. Oligonucleotides were synthesized with the sequence:

5′-(TCCAGNNGCGTC)CTCT-3′, where NN = AT or TA.

The first 4 bases at the 3′-end (CTCT) served to space the oligonucleotide from the surface. Target oligonucleotides were obtained HPLC-purified from Integrated DNA Technologies with the sequences:

5′-(GACGCTACTGGA)TTAC-FAM-3′

5′-(GACGCATCTGGA)TTAC-Cy3–3′.

The target sequences (1 μM in 2× SSC buffer with 0.01% SDS surfactant, Invitrogen) were simultaneously hybridized to the chip for 2 h at room temperature in a humidity chamber. The substrates were washed with 1× SSC with 0.1% SDS, 0.5× SSC, 0.1× SSC, and then dried under nitrogen. Fluorescence images were captured with a Zeiss LSM Pascal confocal microscope.

For the stepwise yield tests, 4 random bases were synthesized using the commercial halo-acid cycle (including capping steps) before any PEC deblock steps. This pre-PEC synthesis procedure limits unrealistically high signal intensity for short oligonucleotides by capping reactive hydroxyls that lack sufficient space to grow into full length strands.

Electrochemical Analysis. Surface potential measurements were measured by contacting a metal line that extended outside a Kalrez o-ring confining the electrolytic solution. Cyclic voltammetry (150 mV/s sweep rate) of 2.5 mM hydrquinone and 100 mM tetrabutylammonium hexafluorophosphate salt in

anhydrous acetonitrile was measured by using a custom-built potentiostat that interfaced with a HP4516A semiconductor analyzer (Fig. S7). A nickel plate (McMaster) and platinum wire (Aldrich) were used as the counter and quasi-reference electrodes of the 3-electrode fluidic, respectively. The substrate was illuminated from the backside using a fiber illuminator as described in *SI Text* (Supporting Note 1).

Porous Glass Characterization. Surface loading experiments were performed on glass slides (Electron Microscopy Sciences) with and without the 840-nm-thick porous glass films. The substrates were amino-silanized with 1% 3-aminopropyltriethoxylsilane in acidic methanol for 30 min. The amine was reacted with 5′-O-DMT-2′-dT-3′-O-succinate (10 mM, Monomer Sciences) and 1,3-dicyclohexylcarbodiimide catalyst (50 mM, Avocado Organics) in anhydrous dichloromethane for 6 h under nitrogen. Trityl loading was determined by treating the substrate with commercial halo-acid deblock solution, and quantifying the DMT cation concentration using a HP8452A spectrophotometer. DNA synthesis capacity was determined by synthesizing a 40mer using the commercial ABI 394 (Applied Biosystems) synthesis cycle in a custom fluidic. The cleaved DNA was quantified using a Nanodrop spectrophotometer after desalting with Microspin G25 columns (GE Healthcare). Denaturing gel electrophoresis confirmed that DNA of the right length was synthesized (Fig. S8).

ACKNOWLEDGMENTS. We thank Scott Manalis and Shuguang Zhang for use of their respective lab facilities, as well as Kurt Broderick, Peter Carr, Jaebum Joo, Manu Prakash, David Kong, David Mosley, and Jason Taylor for technical aid and helpful discussion. This work was funded by the Center for Bits and Atoms (National Science Foundation Grant CCR0122419) and Defense Advanced Research Projects Agency (N66001-05-X6030), and was made possible by the generous donation of the DNA synthesizer by the Massachusetts Institute of Technology Biopolymers Lab.

1. Bard AJ, Stratmann M, Licht S (2002) *Encyclopedia of Electrochemistry* (Wiley-VCH, Weinheim), Vol 6.
2. Sato N (1998) *Electrochemistry at Metal and Semiconductor Electrodes* (Elsevier, New York).
3. Hafeman DG, Parce JW, McConnell HM (1988) Light-sddressable potentiometric sensor for biochemical systems. *Science* 240:1182–1185.
4. Tokudome H, et al. (2005) Photoelectrochemical deoxyribonucleic acid sensing on a nanostructured TiO_2 electrode. *Appl Phys Lett* 87:213901.
5. Chiou PY, Ohta AT, Wu MC (2005) Massively parallel manipulation of single cells and microparticles using optical images. *Nature* 436:370–372.
6. Gurtner C, Edman CF, Formosa RE, Heller MJ (2000) Photoelectrophoretic transport and hybridization of DNA oligonucleotides on unpatterned silicon substrates. *J Am Chem Soc* 122:8589–8594.
7. Hafeman DG, et al. (2006) Optically directed molecular transport and 3D isoelectric positioning of amphoteric biomolecules. *Proc Natl Acad Sci USA* 103:6436–6441.
8. Pappas TC, et al. (2007) Nanoscale engineering of a cellular interface with semiconductor nanoparticle films for photoelectric stimulation of neurons. *Nano Lett* 7:513–519.
9. Colicos MA, Collins BE, Sailor MJ, Goda Y (2001) Remodeling of synaptic actin induced by photoconductive stimulation. *Cell* 107:605–616.
10. Hughes TR, et al. (2001) Expression profiling using microarrays fabricated by an ink-jet oligonucleotide synthesizer. *Nat Biotechnol* 19:342–347.
11. Lausted C, et al. (2004) POSaM: A fast, flexible, open-source inkjet oligonucleotide synthesizer and microarrayer. *Genome Biol* 5:R58.
12. Fodor SP, et al. (1991) Light-directed, spatially addressable parallel chemical synthesis. *Science* 251:767–773.
13. Pease AC, et al. (1994) Light-generated oligonucleotide arrays for rapid DNA sequence analysis. *Proc Natl Acad Sci USA* 91:5022–5026.
14. Singh-Gasson S, et al. (1999) Maskless fabrication of light-directed oligonucleotide microarrays using a digital micromirror array. *Nat Biotechnol* 17:974–978.
15. McGall G, et al. (1996) Light-directed synthesis of high-density oligonucleotide arrays using semiconductor photoresists. *Proc Natl Acad Sci USA* 93:13555–13560.
16. Zhou X, et al. (2004) Microfluidic PicoArray synthesis of oligodeoxynucleotides and simultaneous assembling of multiple DNA sequences. *Nucleic Acids Res* 32:5409–5417.
17. Egeland RD, Southern EM (2005) Electrochemically directed synthesis of oligonucleotides for DNA microarray fabrication. *Nucleic Acids Res* 33:e125.
18. Maurer K, McShea A, Strathmann M, Dill K (2005) The removal of the t-BOC group by electrochemically generated acid and use of an addressable electrode array for peptide synthesis. *J Comb Chem* 7:637–640.
19. Fernandez S, et al. (2007) Combinatorial synthesis of peptide arrays onto a microchip. *Science* 318:1888.
20. Bard AJ, Faulkner LR (2001) *Electrochemical Methods: Fundamentals and Applications* (John Wiley, New York).
21. McGall GH, et al. (1997) The efficiency of light-directed synthesis of DNA arrays on glass substrates. *J Am Chem Soc* 119:5081–5090.
22. Nuwaysir EF, et al. (2002) Gene expression analysis using oligonucleotide arrays produced by maskless photolithography. *Genome Res* 12:1749–1755.
23. Pirrung MC (2002) How to make a DNA chip. *Angew Chem Int Ed* 41:1276–1289.
24. Pirrung MC, Bradley J-C (1995) Comparison of methods for photochemical phosphoramidite-based DNA synthesis. *J Org Chem* 60:6270–6276.
25. Gao X, et al. (2001) A flexible light-directed DNA chip synthesis gated by deprotection using solution photogenerated acids. *Nucleic Acids Res* 29:4744–4750.
26. Kim C, et al. (2006) Progress in gene assembly from a MAS-driven DNA microarray. *Microelectron Eng* 83:1613–1616.
27. Kim C, et al. (2004) Biological lithography: Improvements in DNA synthesis methods. *J Vac Sci B* 22:3163–3167.
28. Livage J, Coradin T, Roux C (2001) Encapsulation of biomolecules in silica gels. *J Phys Condens Matter* 13:R673–R691.
29. Glazer M, Fidanza J, McGall G, Frank C (2001) Colloidal silica films for high-capacity DNA probe arrays. *Chem Mater* 13:4773–4782.
30. Bessueille F, et al. (2005) Assessment of porous silicon substrate for well-characterized sensitive DNA chip implement. *Biosens Bioelectron* 21:908–916.
31. Maurer K, et al. (2006) Electrochemically generated acid and its containment to 100 micron reaction areas for the production of DNA microarrays. *PLoS One* 1:e34.
32. Engels J (1979) Selective electrochemical removal of protecting groups in nucleotide synthesis. *Angew Chem Int Ed* 18:148–149.
33. Kim K, et al. (2002) Electrochemical deprotection for site-selective immobilization of biomolecules. *Langmuir* 18:1460–1462.
34. Hayakawa Y, Kawai R, Wakabayashi S, Uchiyama M, Noyori R (1998) Electrochemical removal of allylic protecting groups in nucleotide synthesis. *Nucleosides Nucleotides* 17:441–449.
35. Franco D, Dunach E (2000) New and mild allyl carbamate deprotection method catalyzed by electrogenerated nickel complexes. *Tetrahedron Lett* 41:7333–7336.
36. Tian J, et al. (2004) Accurate multiplex gene synthesis from programmable DNA chips. *Nature* 432:1050–1054.
37. Cleary MA, et al. (2004) Production of complex nucleic acid libraries using highly parallel *in situ* oligonucleotide synthesis. *Nat Methods* 1:241–248.
38. Saboulard D, et al. (2005) High-throughput site-directed mutagenesis using oligonucleotides synthesized on DNA-chips. *BioTechniques* 39:1–5.
39. Porreca GJ, et al. (2007) Multiplex amplification of large sets of human exons. *Nat Methods* 4:931–936.
40. Albert TJ, et al. (2007) Direct selection of human genomic loci by microarray hybridization. *Nat Methods* 4:903–905.
41. Okou DT, et al. (2007) Microarray-based genomic selection for high-throughput resequencing. *Nat Methods* 4:907–909.
42. Kong DS, Carr PA, Chen L, Zhang S, Jacobson JM (2007) Parallel gene synthesis in a microfluidic device. *Nucleic Acids Res* 35:e61.